# Stochastic cooling experiments for CSRe at IMP

G.Y. Zhu[a,b,c], J.X. Wu[a,c], F. Caspers[d], F. Nolden[e], Y. Zhang[a,c], Y. Wei[a], X.J. Hu[a], Z. Du[a], H.M. Xie[a], L. Jing[a], K.W. Gu[a,c], J.W. Xia[a,c]

[a] Institute of Modern Physics, Chinese Academy of Sciences, Lanzhou 730000, China

[b] University of Chinese Academy of Sciences, Beijing 100049, China
[c] Huizhou Research Center of Ion Sciences, Huizhou 516003, China
[d] CERN, 1211 Geneva 23, Switzerland
[e] GSI Helmholtzzentrum für Schwerionenforschung, Planckstraße 1, 64291 Darmstadt, Germany

**Abstract:** A novel type of perforated travelling wave pick-up/kicker structure was developed for CSRe stochastic cooling which was originally proposed by F. Caspers at CERN. The simulated and measured results of shunt impedance of the slotted travelling wave pickup electrode are in reasonable agreement. In December 2015 stochastic cooling of heavy ions was successfully applied for the first time at the CSRe storage ring of IMP in Lanzhou, China. During four days of commissioning, transverse and longitudinal cooling could be observed. Both the time-of-flight and the notch filter methods were used for longitudinal cooling. The measured cooling rates are presented.
**Key words**: CSRe, Stochastic cooling, pickup/kicker, power amplifier

## 1 Introduction

Stochastic cooling at the experimental Cooler Storage Ring[1], CSRe at the Institute of Modern Physics (IMP) in China, is used mainly for experiments with radioactive fragment beams[2]. They arrive from the separator with momentum spreads and emittances for which electron cooling is too slow. According to the CSRe injection acceptance, CSRe stochastic cooling was designed to cool transverse emittances of up to 20-50 $\pi$ mm. mrad and momentum deviations of up to ±0.5 - 1.0 %. A combination of stochastic precooling and subsequent electron cooling is needed to get overall cooling times of the order of 10 seconds for injected secondary heavy ion beams and beams cooled by electron cooling to equilibrium phase space density. The locations of the pickup and kickers in CSRe are shown in Fig.1. As no straight section is available for the installation of pickups and kickers for stochastic cooling, they have to be installed in the C type bending magnet chambers. The space is very limited inside, vertically only 4 mm were available for the installation of pick-up and kicker electrodes on each side. The choice of appropriate electrode structures was therefore severely limited by these boundary conditions.

In a momentum cooling system, the pick-up signals are combined in sum mode and similarly, the signal to the kicker electrodes is also applied in sum mode, providing longitudinal fields to accelerate or decelerate the passing particles. And betatron or transverse cooling systems use pick-ups in difference mode to generate the beams error signal, then the kickers apply a transverse field to the particles by applying the error signal to the kicker electrodes in "push -pull" fashion (one kicker plate has the same charge to push the beam, the opposing kicker plate has the opposite charge to pull the beam). Fig. 2 is RF signal processing for CSRe stochastic cooling hardware system including momentum and transverse cooling.

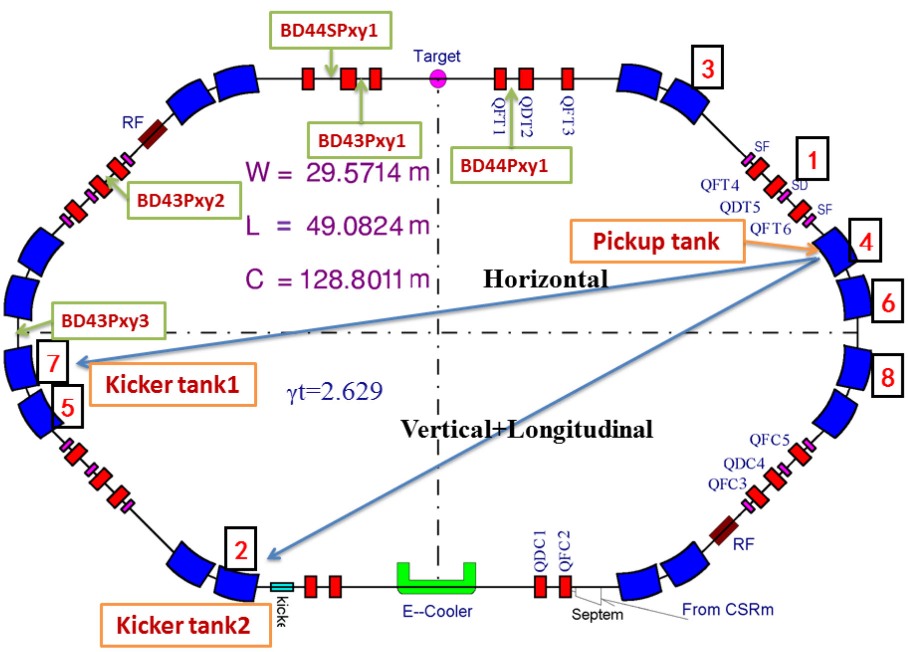


Fig. 1. Layout of stochastic cooling on CSRe. Transverse and longitudinal cooling share one pickup tank. Vertical and longitudinal cooling share one kicker tank.

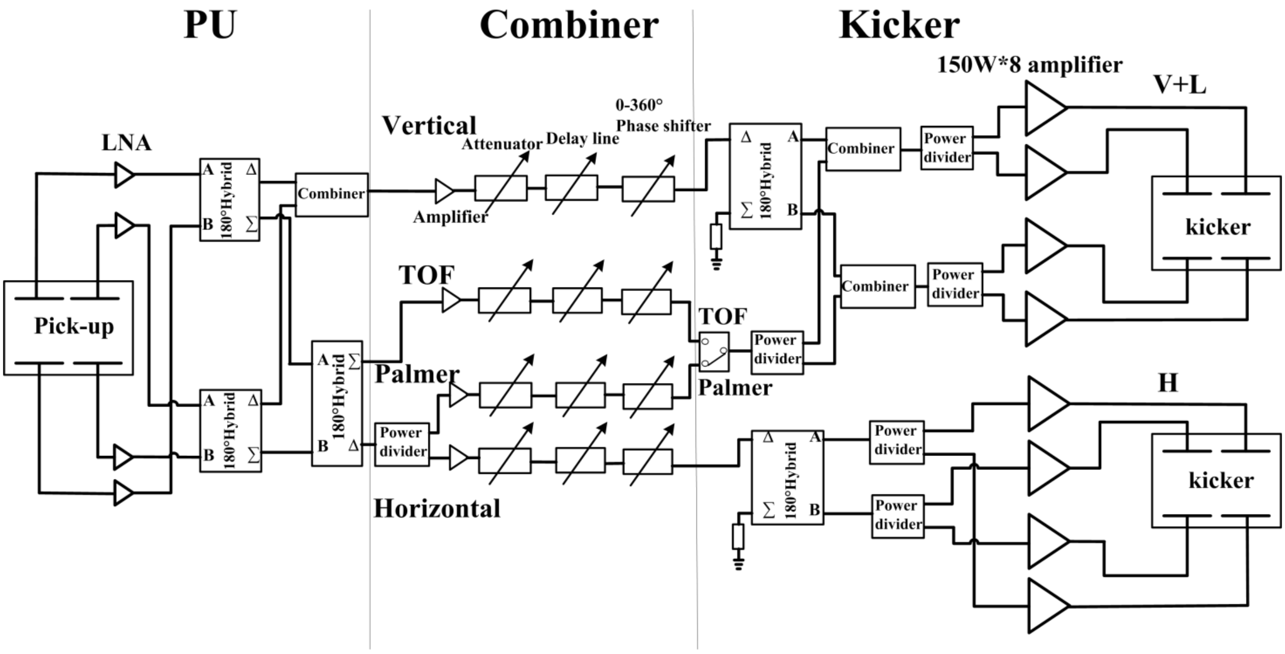


Fig. 2. Stochastic cooling hardware system for CSRe including horizontal, vertical and longitudinal planes. Electronics hardware are mainly distributed in: PU, combiner and Kicker. H, V and L indicate horizontal, vertical and longitudinal respectively.

## 2 Acceptance

For the longitudinal cooling, the synchronization error due to undesired mixing between pickup and kicker is due to a timing error relative to the reference particle

$$\frac{\delta T}{T_{p\to k}} = -\eta\frac{\Delta p}{p} + \alpha_p\frac{\delta\left(\frac{m}{q}\right)}{\left(\frac{m}{q}\right)} \qquad (1)$$

for different beams with different mass to charge ratio $m/q$, where $T_{p\to k}$ denotes the time of flight from pickup to kicker, $\alpha_p$ is the momentum compaction, $\eta = \gamma^{-2} - \alpha_p$ is the frequency slip factor. For just one beam, the second term in the formula is 0. The longitudinal TOF cooling force will scale as

$$F_{\parallel} \propto \sum_m G \cdot \sin\left(m\omega_0 T_{p\to k}\eta\frac{\Delta p}{p}\right) \quad (2)$$

if the system is tuned to the reference particle. G includes the transmission gain from pickup to kicker, the frequency response of pickups and kickers, and m is the harmonic number. The sum is over the harmonic of the revolution frequency inside the cooling bandwidth. It can be clearly seen that for too large momentum spread, the cooling force changes sign, i.e. heats up the beam. This is illustrated in Fig. 3 where the drift term is displayed for different momentum deviation for CSRe longitudinal stochastic cooling with bandwidth from 100 MHz to 600 MHz and with TOF method. For TOF cooling the acceptance is about ±1.36 %, which is larger than the maximum beam spread ±1.0 %.

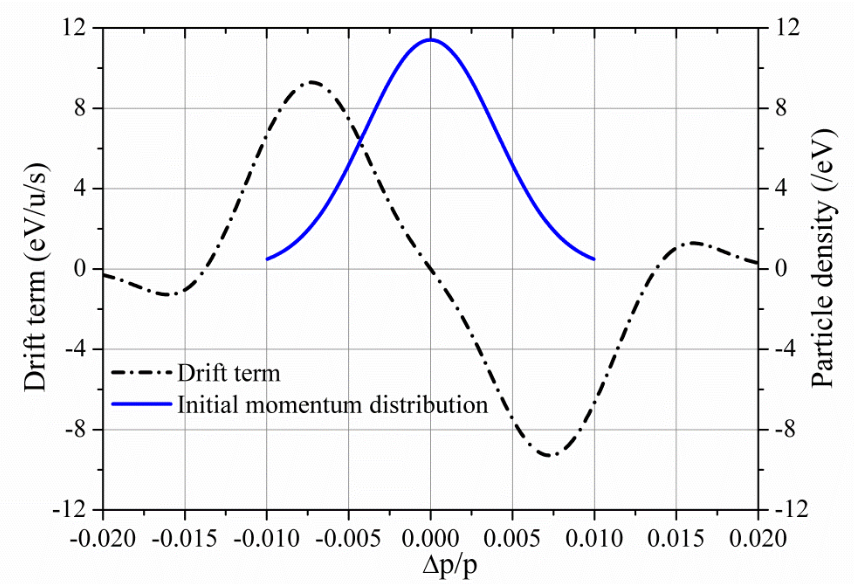


Fig. 3. The drift term as a function of momentum deviation for CSRe TOF cooling (black dotted curve) and initial momentum distribution (blue curve)

## 3 Pick-up/kicker

### 3.1. Structure and dimension

A novel type of perforated travelling wave pick-up/kicker structure was developed for CSRe stochastic cooling which was originally proposed by F. Caspers at CERN in 1998[3], shown in Fig. 4. Four electrodes are installed inside the beam tube to give the beam positions or provide the excitations. The electrodes are bent according to the geometry inside the vacuum chamber of the dipole magnets, being 87 mm wide and 2.76 m long. They are supported and fixed by many ceramic cylinders inside the beam tube. Two feedthrough ports are mounted at each end of the electrode, one for signal output and one for load. They are easily accessible outside the magnet structure. The thickness of the electrode metal foil amounts to 0.4 mm and the distance from the electrode to the ground is 3 mm. The distribution of the electrodes inside the vacuum tube is shown in Fig. 5. A detailed description of the perforated structure can be found in Refs. [4] and [5].

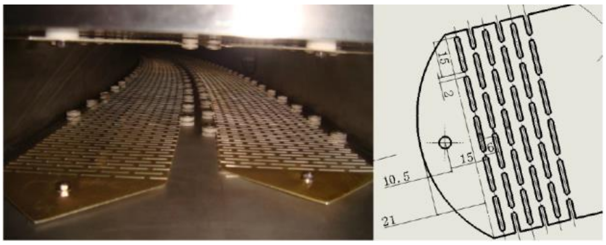

Fig. 4. The slotted stripline electrode inside the bending vacuum tube

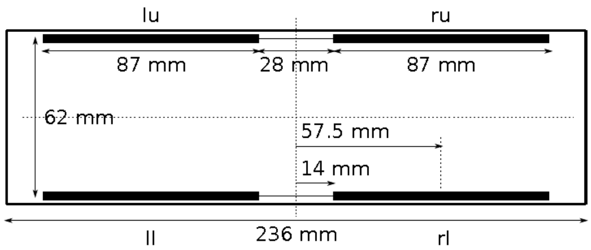


Fig. 5. The layout of the electrodes inside the vacuum tube

### 3.2. Beta value and attenuation measurement

A large number of small slots in this electrode provide distributed inductive loading, slowing down the phase velocity of the travelling wave structure. The reduction in phase velocity is a function of the slot length, slot width, electrode thickness, and the spacing between the electrode and ground. This kind of inductive loading, using a large number of rather small slots is applicable for a velocity range $\beta$ =v/c from about 0.5 to 0.95. But for a given structure the momentum range is rather narrow. In our case, the optimum stochastic cooling was designed for the beam energy of 400 MeV/u, so the perforated structure was optimized to match this value. The phase velocity is measured using the resonant method [6], and the measurement results are shown in Fig. 6. The phase velocity variations are very likely due to the fact that the electrode is not flat after installation, also the gap between the electrode and the ground is not exactly the same for each electrode. After manufacturing the perforated copper electrode, about a 20 micron silver layer with a flash of gold was coated on it to minimize the attenuation. We compared the attenuation with and without silver and gold coated for the same electrode, as shown in Fig. 7. It is clear that the electrode attenuation is decreased with silver and gold plated. So it can be used as kicker structures without any significant power dissipation inside the vacuum tube.

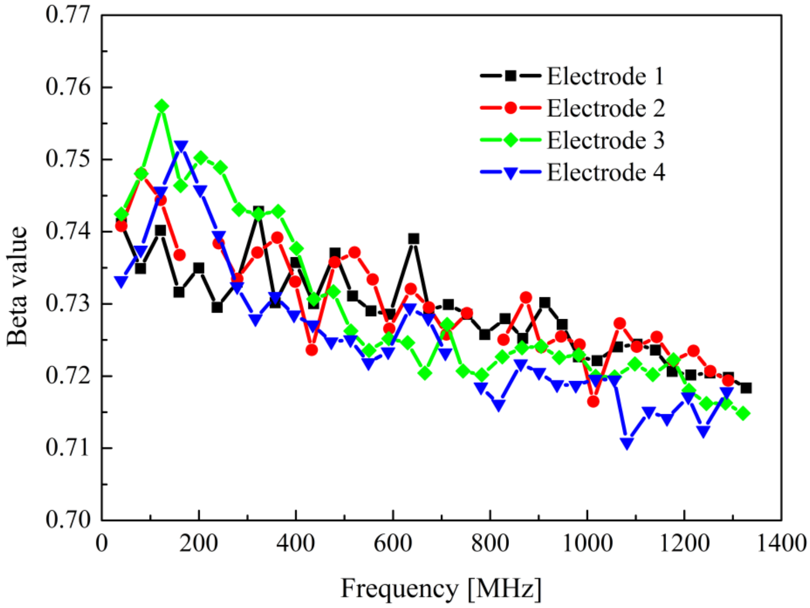


Fig. 6. Phase velocity measurement.

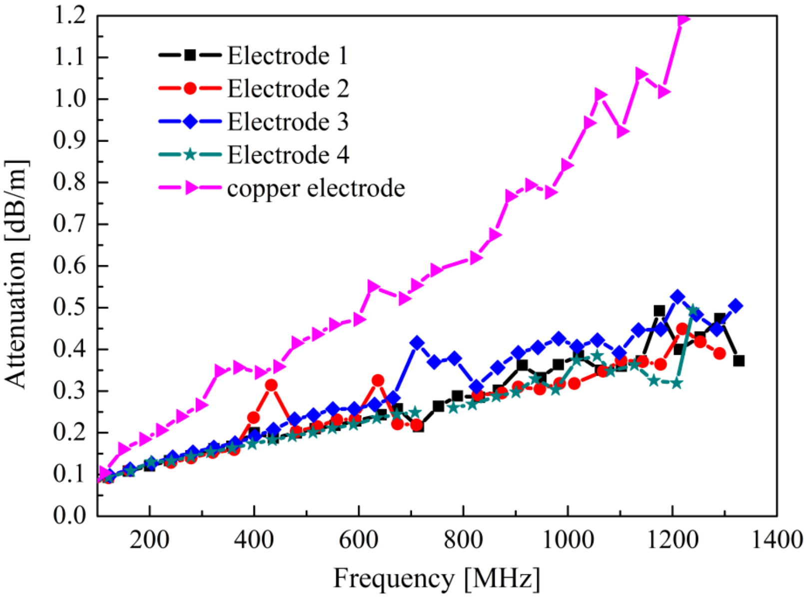


Fig. 7. Attenuation measurement on a test bench.

3.3. Phase dispersion measurement

In contrast to other similar looking electrodes (Faltin type pick-up [7], McGinnis type slotted waveguide structure for beta=1 [8]) this device is very broadband and operates from low frequencies onwards as a forward coupler. Due to the small size of the slots the frequency dependency of the inductance of these slots is very low, leading to a small dispersion over a large frequency range. The phase response measurement of the 2.76 m long electrode is shown in Fig. 8. Below 1.2 GHz the difference from linear phase is never more than 45 degrees. Thus, in a frequency range from a few MHz to 1.2 GHz the structure has a phase dispersion acceptable for CSRe stochastic cooling. Because of its rather good phase response, it can be made very long to overcome the problems of intermediate signal feedthroughs. Also because it is a forward travelling wave structure, the coupling impedance is proportional to the square of the length and it is really becoming good for a considerable length. Of course this is in conflict with the beta variation range.

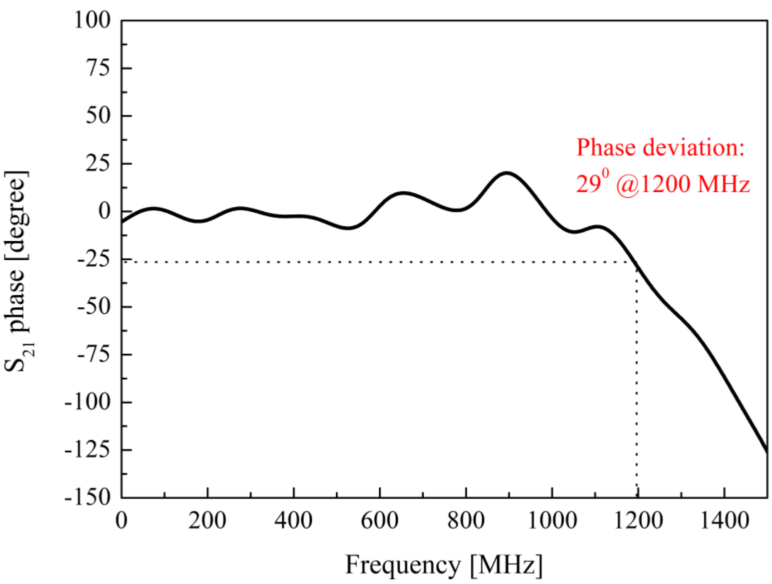


Fig. 8. Phase dispersion measurement on a test bench.

3.4. Shunt impedance simulation and measurement

According to the definition of D.A.Goldberg[9], for N particles with the charge state of q and revolution frequency of $f_0$, the Schottky power from the pickup signal into an impedance-matched load $Z_c$ at each harmonic is

$$P_{sch} = (I^2) \cdot Z_{PU}^2/Z_c = 2N \cdot (qef_0)^2 \cdot Z_{PU}^2/Z_c \quad (3)$$

where $Z_{PU}$ is the transfer impedance of the pickup electrode which is a function of frequency and beam energy, and $Z_{PU}^2/Z_c$ is the pickup shunt impedance. Fig. 9 is the comparison of $Z_{PU}^2/Z_c$ between the simulation result with HFSS (High Frequency Structure Simulator) [10] and the beam measurement with a $^{78}Kr^{36+}$ beam with an energy of 308 MeV/u. The measured result has many resonances/spikes which are caused by the impedance mismatch from 16 Ω to 50 Ω of the signal transmission, as the characteristic impedance of the pickup structure amounts to about 16 Ω because of space limit between the electrode and ground. The simulated result has higher coupling impedance as dissipation by the electrode itself, the impedance mismatch, and so on, are not considered in the simulation. At higher frequency the measured result deviates from the simulation because of poor signal to noise ratio, as for high harmonics, the Schottky power spectral density decreases. But anyway the measured and simulated result has some agreement, and to some extent the simulation is reliable.

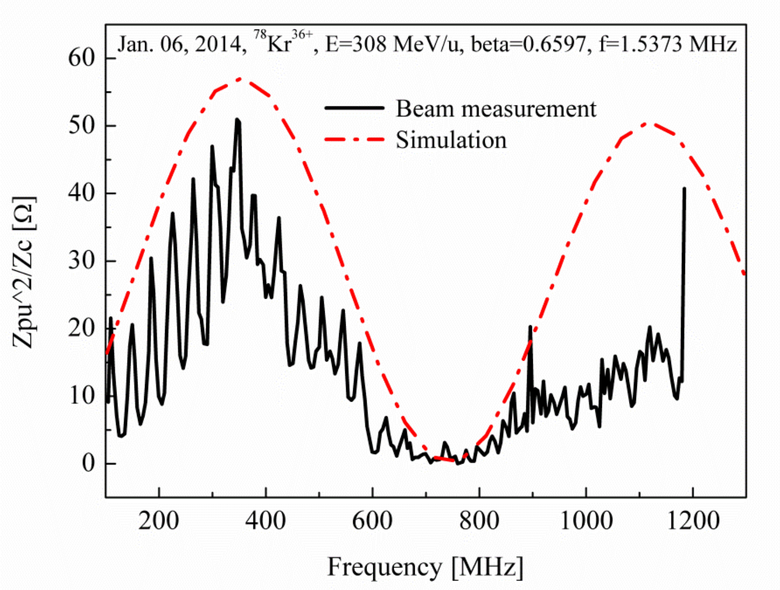


Fig. 9. Comparison of $Z_{PU}^2/Z_c$ with simulation and beam measurement

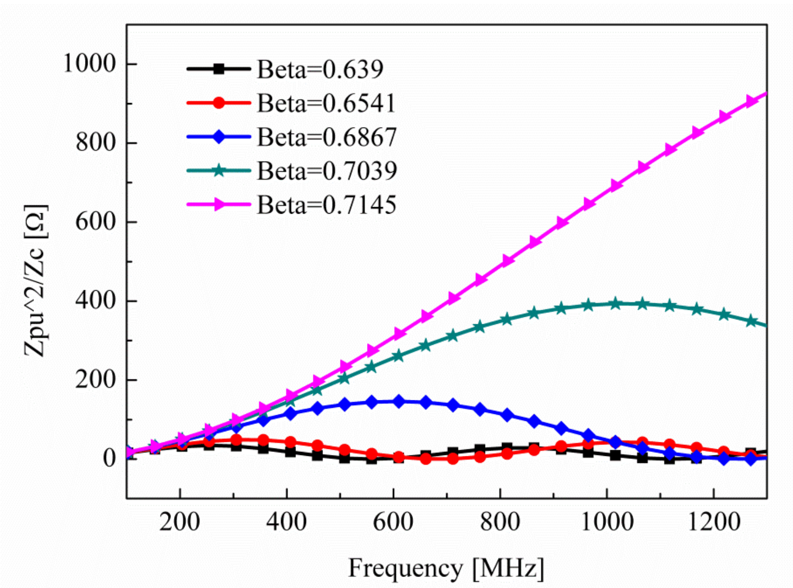


Fig. 10. Simulated coupling impedance for different beam energy

Fig. 10 shows the simulated pick-up shunt impedances for different beam energies. The wave in the pickup induced by the beam travels parallel to the beam and at the same velocity such that induction from beam to stripline through each slot adds constructively. Therefore, in this traveling wave pickup, it is crucial that the phase velocity in the stripline approximately equals the particle velocity across the desired frequency band of operation. Fig. 11 is the HFSS simulation model and the size of the model can be found in Fig. 5. As a result of this simulation it follows that such a long electrode can hardly be used for the beam energy below 350 MeV/u, it works best for beam energies in the range 380 MeV/u - 400 MeV/u. The energy 400 MeV/u is close to the optimum energy.

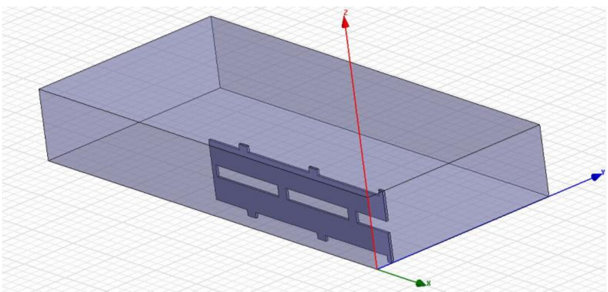

Fig. 11. HFSS simulation model

## 4 Power amplifier

According to the simulation using the Fokker-Planck equation[11], for high charge-stated beam with small particle number less than $1.0*10^5$, like $^{132}Sn^{50+}$ and $^{238}U^{92+}$, the cooling speed is fast enough with the gain of 134 dB, which means the noise power is less than 150 W. Fig.12 is the simulated result of Palmer cooling for a $^{132}Sn^{50+}$ beam with particle number of $1.0*10^5$. The noise is within 110 W. But for low charge state beam with large particle number, like $^{36}Ar^{18+}$ with particle number of $5.0*10^6$, it is better with the gain of 138 dB, which means the noise power is about 250 W. The simulated results are shown in Fig.13 and Fig.14. To account for losses in the cooling chain and for the statistical nature of the cooling signals a safety factor 4 to 6 has to be included to avoid signal distortions due to e.g. amplifier non-linearities so that the necessary electronic power is 4-6 times of the noise power [12]. This guarantees that the amplifiers will not be saturated and no additional heating is introduced. Presently we reserved the RF power of 600 W for the longitudinal cooling, each electrode with 150 W. For high charge-stated beam with small particle number, the power is enough. But for large particle number, the system will work in power limited situation.

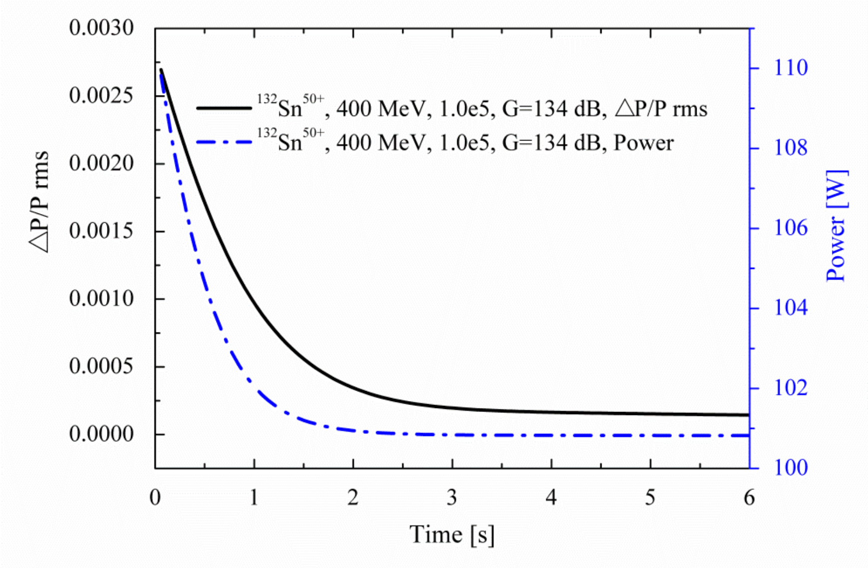


Fig. 12. Longitudinal momentum cooling and total noise power for beam $^{132}Sn^{50+}$

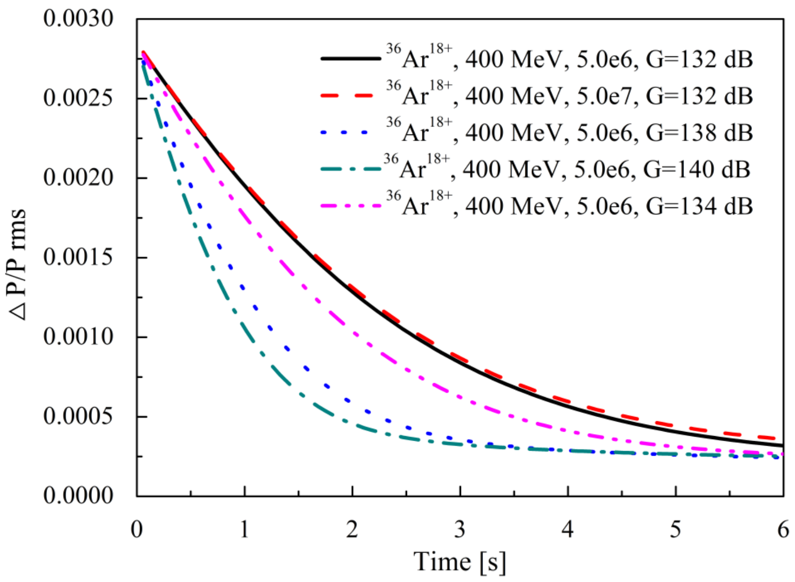


Fig. 13. Longitudinal momentum cooling for beam $^{36}Ar^{18+}$

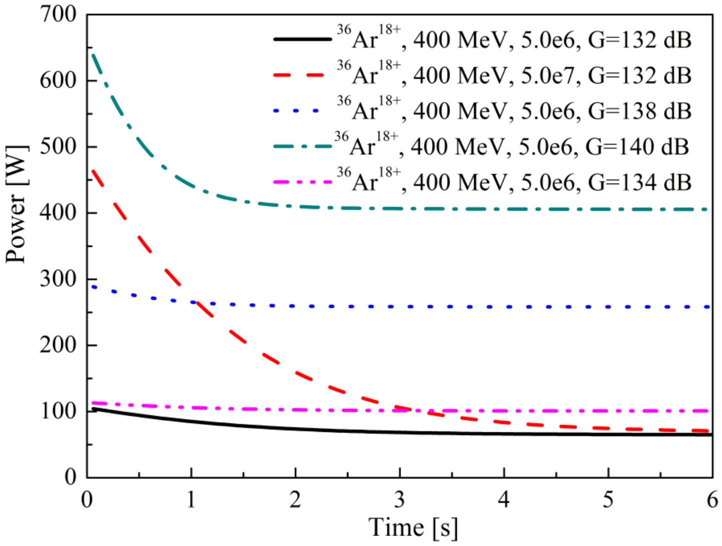


Fig. 14. Total noise power for beam $^{36}Ar^{18+}$

In the simulation, the bandwidth is 100 - 600 MHz. Basically, the pickup/kicker structure and other hardware components can be used up to 1 GHz. A transmission measurement of a lengthy part of the CSRe vacuum tube (Fig. 15) resulted in a cutoff frequency of about 650 MHz. To avoid the installation of attenuating material in the CSRe to dissipate the unexpected propagation, and to do the stochastic cooling step by step to make things more easy and reasonable, we decided to perform the cooling in two phases. Phase 1 is with the bandwidth of 100 MHz-600 MHz and phase 2 is 200 MHz-1200 MHz.

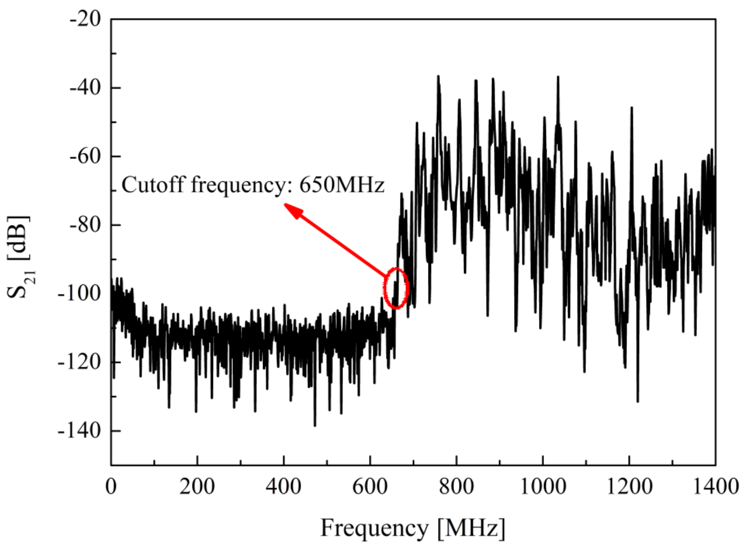


Fig. 15. Transmission measurement of the CSRe beam tube

To ensure that the correcting signal and the beam arrive at the same time at the kicker, too long transmission cables must be avoided. For the cooling loop, the time delay in the coaxial cable from the pickup to kicker is about 151 ns. For the beam with energy of 400 MeV/u, the time of flight from pickup to kicker is 217 ns. Then only 66 ns are left for the delay inside electronic devices. Therefore the time delay inside the power amplifier should be as short as possible and it is required to be within 15 ns. The data of the purchased power amplifier basically fit all our requirements and the delay is less than 15 ns. The transmission measurement of the power amplifier is shown in Fig.16. The gain flatness below 1 dB compression is ±2 dB and the phase variation is ±10 degrees. The output power at P1dB (1 dB compression point) is 150 W for one module.

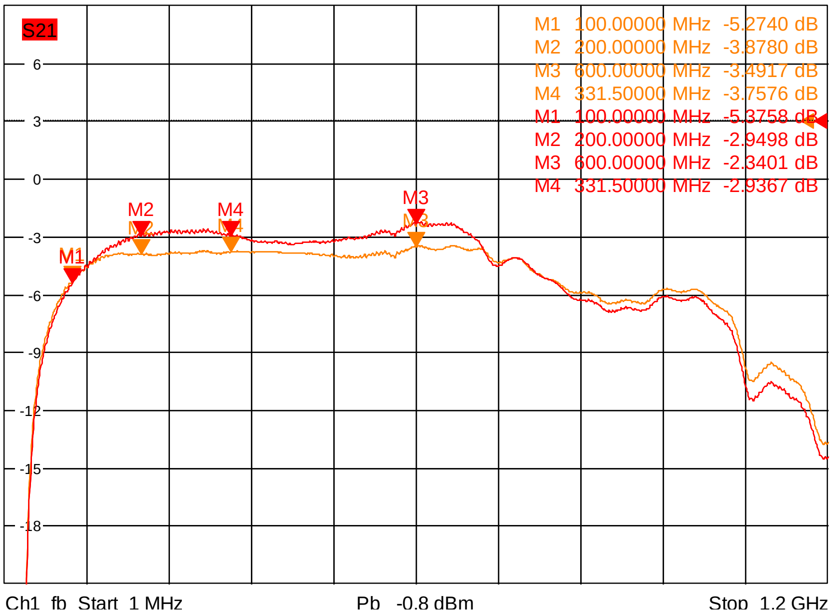


(a) gain measurement with 57dB coupler

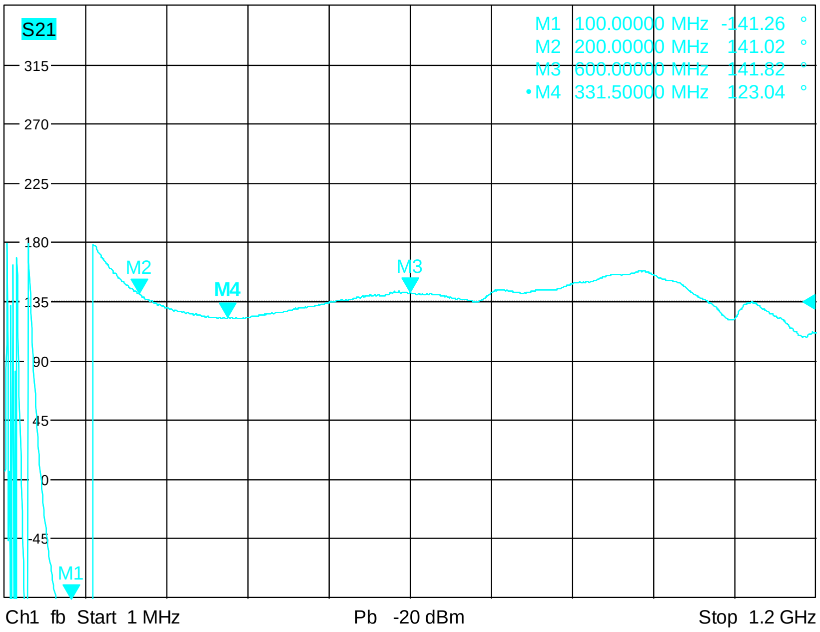


(b) phase measurement

Fig. 16. Transmission of the Power amplifier

## 5 Stochastic cooling experiments on CSRe

In Dec. 2015, for the first time stochastic cooling beam experiments were performed at CSRe for a $^{12}C^{6+}$ beam with an energy of 380 MeV/u. The longitudinal Schottky spectra in Fig.17 represent the momentum distribution at different times during the stochastic cooling experiment with TOF method for particle number of 7.0E7. Before cooling the momentum spread (rms) is 8.0E-4, after 130 s with stochastic cooling on the momentum spread is decreased to 3.0E-4. The initial momentum spread was small because the beam was already cooled by electron cooling inside CSRm before it was injected into CSRe.

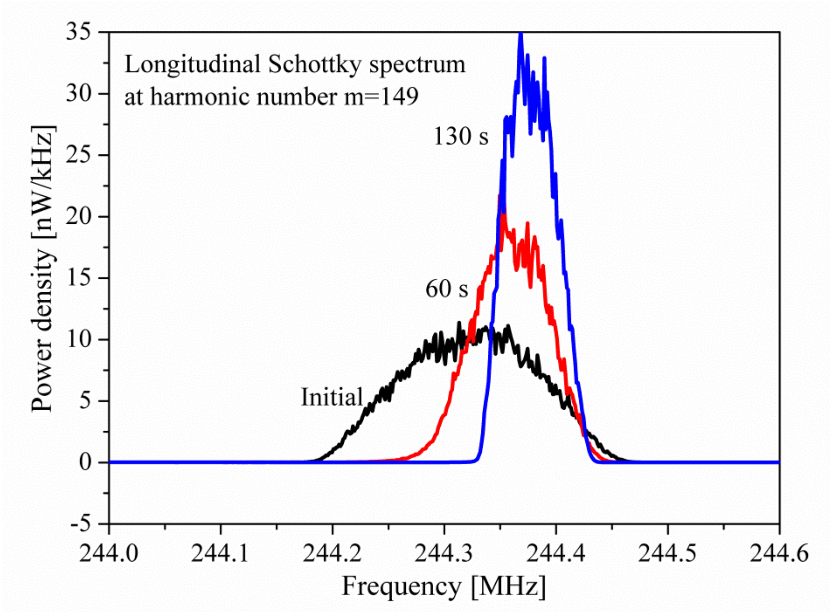


Fig. 17. Longitudinal stochastic cooling experiment with TOF method.

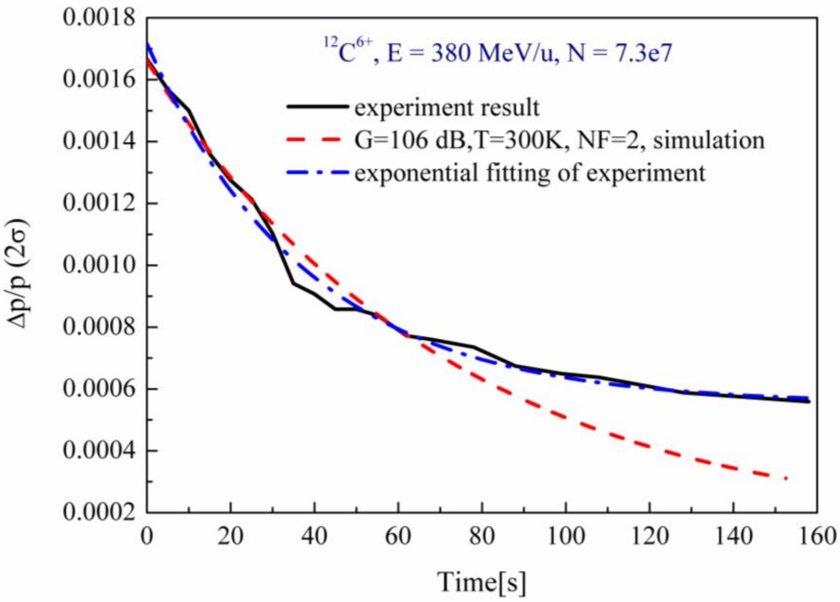


Fig. 18. Comparison of Experiment & simulated result for longitudinal stochastic cooling

Fig.18 is the comparison between the simulation and beam experiment in Fig.17. The parameters in the simulation are shown in table 1. At the beginning of the cooling, the simulation and the experiment have good agreement, but in the end, they are far from each other. The equilibrium momentum spread from the experiment is much larger than the simulation. It implies that the most obvious reason for this discrepancy is the impedance mismatch between the structure inside the vacuum chamber and the 50 Ω electronics outside.

Table 1. The parameters in the simulation of CSRe stochastic cooling.

| Parameters | Numerical values |
|---|---|
| Beam | $C^{6+}$ |
| Energy | 380MeV/u |
| Particle number | $7.0*10^7$ |
| Initial momentum spread (rms) | $\Delta p/p=\pm 8.0*10^{-4}$ |
| CSRe circumference | 128.8 m |
| Distance from pickup to kicker | 46.6 m |
| Electrode length | 2.76 m |
| Phase velocity of electrode | 0.72 |
| Bandwidth | 100 MHz – 600 MHz |
| Gain | 106 dB |
| Transition energy $\gamma_t$ | 2.629 |
| Dispersion at pickup/kicker | 6.15 m/0.8 m |

For horizontal cooling, only two units of the power amplifier are installed, i.e. the CW power of the horizontal cooling is only 300 W. After the output of each power amplifier, the power is divided to two electrodes. Fig.19 is the spectrogram of the horizontal signal, originating from the difference of the inner and outer electrodes, during the horizontal cooling with particle number of $2.37*10^7$. As the beam was not centered correctly in the pickup, the longitudinal Schottky signal was not rejected which is shown on the left side of the spectrogram, and the signal on the right side is the transverse sidebands. The Q value is 2.56 therefore the two sidebands partly overlap. On the spectrogram because of the poor signal to noise ratio, the cooling cannot be observed very well like the longitudinal cooling. But when the two spectra at time 0 and 6 seconds later are compared, which is shown in Fig.20, it is clearly seen that the transverse sidebands are decreased which demonstrated transverse cooling. The area of the longitudinal Schottky bands remains unchanged, which means no beam loss during the transverse cooling. This is also proved by the beam transformer measurement. As no quantitative emittance measurements were performed during the experiment, we cannot judge how much the transverse emittance was decreased. When the power of the sidebands over frequency range of 297.25 MHz – 298.25 MHz is integrated for each spectrum, which is shown in Fig.21, the power of the transverse sidebands is decreased by 20% in 5 s.

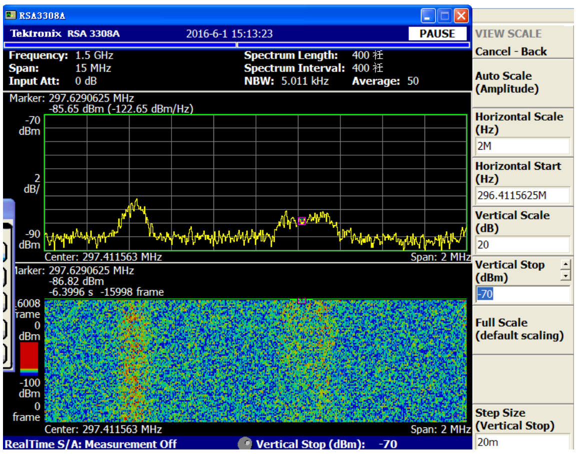


Fig. 19. Transverse stochastic cooling experiment, where the yellow curve is the horizontal signal which is the difference from the inner and outer electrodes.

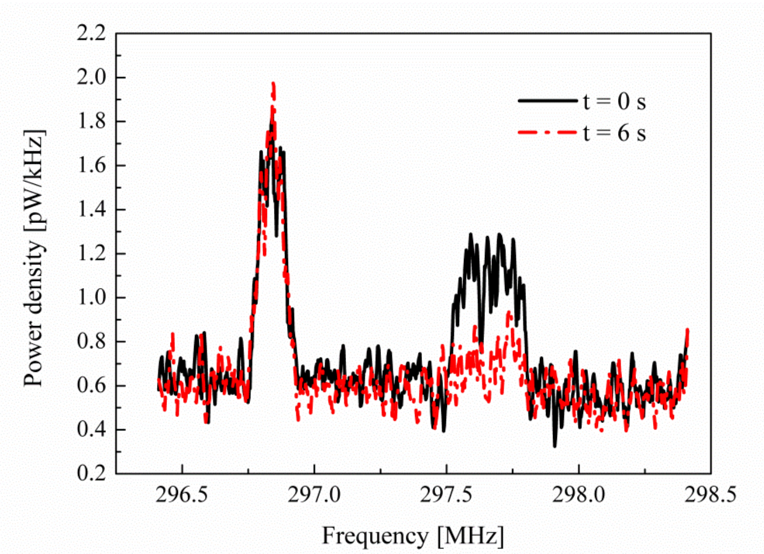


Fig. 20. Transverse sidebands at different times

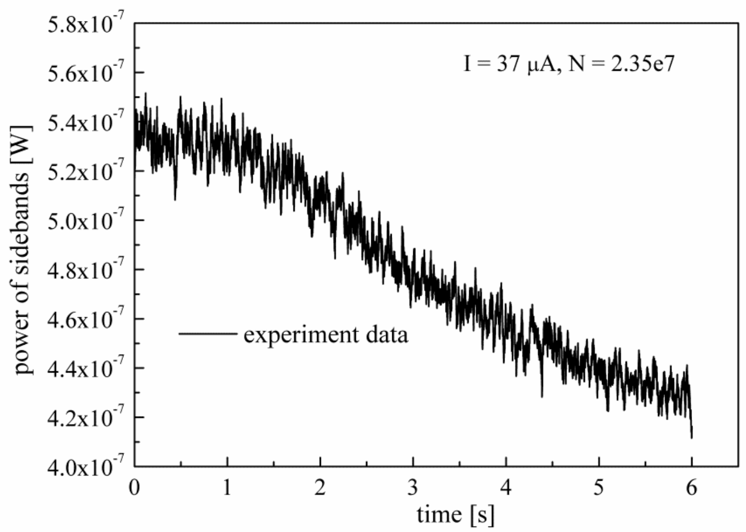


Fig. 21. Power of sidebands during transverse cooling

## 6 Summary

Stochastic cooling both in transverse and longitudinal was just demonstrated at CSRe. The system needs to be improved at some aspects, for example more gain of the cooling loop, the impedance mismatch problem, very deep notch filter and so on. Some of them are undergoing and some of them have been finished. In the end of 2018, the cooling the system is planned to be used for experiments with secondary beams.

## Acknowledgements

*We would like to thank Lars Thorndahl and Takeshi Katayama who gave us strong support all those years.*

*This work was supported by National Natural Science Foundation of China (No. 11505259) and Guangdong Innovative and Enterpreneurial Research Team Program (Grant No. 2016ZT06G373).*

## Reference

[1] J. W. Xia, W. L. Zhan, B. W. Wei et al. The heavy ion cooler-storage-ring project (HIRFL-CSR) at Lanzhou. Nucl. Instrum. Methods. A, **488**:11-25 (2002)

[2] Xia Jiawen, Yuan Youjin, Liu Yong, et al. HIRFL-CSR commissioning in 2006 and 2007. Chinese Physics C, 2009, 33(Suppl.Ⅱ): 17-19.

[3] F.Caspers, A novel type of forward coupler slotted strip-line pickup electrode for non-relativistic particle beams, ATS/Note/2011/075(TECH), 2011-09-09.

[4] J.X. Wu, Y. Zhang, G.Y. Zhu, et al. A Novel Type of Forward Coupler Slotted Stripline Pickup Electrode for CSRe Stochastic Cooling. Proceedings of IPAC2013, Shanghai, China 571-573 (2013)

[5] J.X. Wu, Y.Zhang, L.Ming et al. Stochastic Cooling Project at the Experimental Storage Ring CSRe at IMP. Proceedings of COOL'11, Alushta, Ukraine 64-66 (2011)

[6] T. Kroyer. F. Caspers, E. Gaxiola, Longitudinal and Transverse Wire Measurements for the Evaluation of Impedance Reduction Measures on the MKE Extraction Kickers, 2007, CERN-AB-Note-2007-028

[7] L. Faltin, Slot-type pick-up and kicker for stochastic beam cooling, Nucl. Instr. And Meth. 148(3), (1978) 449-455.

[8] D. McGinnis, et al., Slotted waveguide slow-wave stochastic cooling arrays, Proceedings of the 1999 Particle Accelerator Conference, New York, 1999.

[9] Goldberg D A, Lambertson G R. Dynamic devices: A primer on pickups and kickers. American Institute of Physics, 537-600 (2008)

[10] http://www.ansys.com/ (2016).

[11] Dieter Möhl, Stochastic cooling of particle beams, Lecture notes in Physics 866, Springer, (2013)

[12] Hans Stockhorst, Takeshi Katayama, Rudolf Maier. Beam cooling at COSY and HESR. Schlusseltechnologien Key Technologies. Band/Volume 120. ISBN 978-3-95806-127-9 (2016)